AFRL-RI-RS-TR-2018-079

COOPERATIVE ROUTING FOR DYNAMIC AERIAL LAYER NETWORKS

THE UNIVERSITY OF KANSAS CENTER FOR RESEARCH, INC.

MARCH 2018

FINAL TECHNICAL REPORT

APPROVED FOR PUBLIC RELEASE; DISTRIBUTION UNLIMITED

STINFO COPY

AIR FORCE RESEARCH LABORATORY
INFORMATION DIRECTORATE

■ **AIR FORCE MATERIEL COMMAND** ■ **UNITED STATES AIR FORCE** ■ **ROME, NY 13441**

NOTICE AND SIGNATURE PAGE

AFRL-RI-RS-TR-2018-078 HAS BEEN REVIEWED AND IS APPROVED FOR PUBLICATION IN ACCORDANCE WITH ASSIGNED DISTRIBUTION STATEMENT.

FOR THE CHIEF ENGINEER:

/ S /
MICHAEL J. MEDLEY
Work Unit Manager

/ S /
JOHN D. MATYJAS
Technical Advisor, Computing
& Communications Division
Information Directorate

REPORT DOCUMENTATION PAGE

Form Approved
OMB No. 0704-0188

1. REPORT DATE *(DD-MM-YYYY)*	**2. REPORT TYPE**	**3. DATES COVERED** *(From - To)*
MAR 2018	FINAL TECHNICAL REPORT	FEB 2014 – SEP 2017

4. TITLE AND SUBTITLE
COOPERATIVE ROUTING FOR DYNAMIC AERIAL LAYER NETWORKS

5a. CONTRACT NUMBER FA8750-14-1-0077
5b. GRANT NUMBER N/A
5c. PROGRAM ELEMENT NUMBER 62702F

6. AUTHOR(S)
Lingjia Liu

5d. PROJECT NUMBER T2CD
5e. TASK NUMBER KU
5f. WORK UNIT NUMBER LL

7. PERFORMING ORGANIZATION NAME(S) AND ADDRESS(ES)
The University of Kansas Center for Research, Inc.
2385 Irving Hill Road
Lawrence KS 66045-7568

8. PERFORMING ORGANIZATION REPORT NUMBER

9. SPONSORING/MONITORING AGENCY NAME(S) AND ADDRESS(ES)
Air Force Research Laboratory/RITF
525 Brooks Road
Rome NY 13441-4505

10. SPONSOR/MONITOR'S ACRONYM(S) AFRL/RI
11. SPONSOR/MONITOR'S REPORT NUMBER AFRL-RI-RS-TR-2018-079

12. DISTRIBUTION AVAILABILITY STATEMENT
Approved for Public Release; Distribution Unlimited. This report is the result of contracted fundamental research deemed exempt from public affairs security and policy review in accordance with SAF/AQR memorandum dated 10 Dec 08 and AFRL/CA policy clarification memorandum dated 16 Jan 09

13. SUPPLEMENTARY NOTES

14. ABSTRACT
Future Air Force networks will face the challenge of providing robust data and circuit services to tens or hundreds of fixed and mobile users with different service levels. Some of the service challenges include guaranteed rates, communication over difficult channels, hard time-deadlines, reliable message delivery over unreliable networks, security, and policy-driven resource allocation. In light of the propagation characteristics as well as the new challenges of the aerial layer communications, the project “Cooperative Routing for Dynamic Aerial Layer Networks” is funded by Air Force Research Laboratory (AFRL) under grant number FA8750-14-1-0077 to develop a novel and fundamental framework on which new enabling aerial layer communication technologies and protocols can be designed and analyzed. To be specific, the project 1) focuses on dynamic spectrum access (DSA) networks which efficiently allow different wireless nodes to co-exist in the same radio spectrum; 2) introduces a new cooperative aerial layer routing strategy based on mutual-information accumulation (e.g., rateless codes, fountain codes, and hybrid ARQ); 3) develops dynamic network resource management and collaborative routing strategies in support of joint aerial layer networking (JALN) concept; and 4) demonstrates the effectiveness of the strategies introduced using Ettus universal software radio peripheral (USRP) N210s. Our analytical results show that both the centralized and distributed algorithms can reduce up to 77% of the end-to-end delay compared to the traditional routing strategies in DSA networks; demo results using USRP N210s confirm analytical findings.

15. SUBJECT TERMS
Dynamic spectrum access, cognitive radio network, cooperative routing, rateless coding and spectrum underlay

16. SECURITY CLASSIFICATION OF:			**17. LIMITATION OF ABSTRACT**	**18. NUMBER OF PAGES**	**19a. NAME OF RESPONSIBLE PERSON**
a. REPORT	**b. ABSTRACT**	**c. THIS PAGE**			MICHAEL J. MEDLEY
U	U	U	UU	46	**19b. TELEPHONE NUMBER** (*Include area code*)

Standard Form 298 (Rev. 8-98)
Prescribed by ANSI Std. Z39.18

TABLE OF CONTENTS

LIST OF FIGURES

1.0 EXECUTIVE SUMMARY

1.1 Overview of the Project

Future Air Force networks will face the challenge of providing robust data and circuit services to tens or hundreds of fixed and mobile users with different service levels. Some of the service challenges include guaranteed rates, communication over difficult channels, hard time-deadlines, reliable message delivery over unreliable networks, security, and policy-driven resource allocation.

In light of the propagation characteristics as well as the new challenges of the aerial layer communications, the project "Cooperative Routing for Dynamic Aerial Layer Networks" is funded by Air Force Research Laboratory (AFRL) under grant number FA8750-14-1-0077 to develop a novel and fundamental framework on which new enabling aerial layer communication technologies and protocols can be designed and analyzed. To be specific, the project 1) focuses on dynamic spectrum access (DSA) networks which efficiently allow different wireless nodes to co-exist in the same radio spectrum; 2) introduces a new cooperative aerial layer routing strategy based on mutual-information accumulation (e.g., rateless codes, fountain codes, and hybrid ARQ); 3) develops dynamic network resource management and collaborative routing strategies in support of aerial layer networking; and 4) demonstrates the effectiveness of the strategies introduced using Ettus universal software radio peripheral (USRP) N210s. Our analytical results show that both the centralized and distributed algorithms can reduce up to 77% of the end-to-end delay compared to the traditional routing strategies in DSA networks; demo results using USRP N210s confirm analytical findings.

1.2 List of People Involved

There is one faculty member and three Ph.D. students involved in the project, which are listed in the following:

- Lingjia Liu; University of Kansas (KU); PI
- Hao Chen; University of Kansas (KU); Ph.D. student investigator
- Rachad Atat; University of Kansas (KU): Ph.D. student investigator
- Somayeh (Susanna) Mosleh; University of Kansas (KU): Ph.D. student investigator

It is important to note that both Hao and Rachad defended their Ph.D. in June 2017 with help from the grant.

2.0 INTRODUCTION

In the Air Force's network-enabled paradigm, many capabilities will be generated through, and dependent on, the integrated efforts of multiple components. In general, robust dynamic tactical networks can support 10,000 to 500,000 communicating devices in theater, going beyond traditional tactical networks, oriented to the voice and human users, and beyond traditional ad hoc networks. Furthermore, the Air Force network must provide robust data and circuit services to tens or hundreds of fixed and mobile users with different service levels. Some of the service challenges include guaranteed rates, communication over difficult channels, hard time-deadlines, reliable message delivery over unreliable networks, security, and policy-driven resource allocation. These characteristics are primarily driven by defense needs.

In response to challenges associated with the current and anticipated Air Force network, the concept of aerial layer networking is introduced. The aerial layer provides a new horizon for aerial wireless communications. By utilizing aerial layer assets as communications nodes and relays, the Air Force and its partners can readily amplify and augment available communications assets and enhance warfighter collaboration. Using the aerial layer, communications assets are not constrained by terrestrial topology and the limitations hindering ground and space-based communications. Instead, the aerial layer enables dynamic network topology changes, increases bandwidth on-the-fly, and, additionally, alternates routing for existing communications networks to reduce enemy threats.

Dynamic spectrum access (DSA), also known as Cognitive Radio Network (CRN), has been regarded as one of the key techniques to improve the spectral efficiency of a wireless network. The basic idea of DSA is to allow secondary users (SUs) to use primary user (PU) spectrum under the condition that SUs will not cause unacceptable interference to PUs. Several approaches have been introduced on how SUs should access the licensed spectrum such as spectrum overlay [Liang2008Sensing] [Rem2014Cad], spectrum underlay [Sharma2008Channel] or cooperation [Su2010Active]. Overlay approaches enable SUs transmit only when PUs are sensed as idle. Underlay approaches allow SUs to coexist with PUs under the constraint that SU's interference to PUs is under a certain threshold. For cooperation approaches, SUs act as a relay to collaborate with the PUs.

In underlay DSA networks, SUs and PUs are transmitting simultaneously on the same radio spectrum. In order to make sure that the interference from SUs to PUs is tolerable, SUs are usually required to transmit at a low power level resulting in a rather limited link coverage. To address this issue, in this project, we introduce cooperative routing strategies among SUs to extend SU network coverage. To be specific, we consider a SU network that employs advanced channel coding strategies such as mutual-information accumulation at the physical layer, and study the cooperative routing and resource allocation problems associated with such SU networks.

Rateless codes are an advanced technique compared with fixed-rate codes and a realistic method to realize mutual-information accumulation in the physical layer. With a fixed-rate code, the transmitter needs to design codes based on the dynamic channel state information (CSI), often incurring resource waste or too many errors. To guarantee reliable transmission, the data length and number of redundancy bits are always long, decreasing the transmission efficiency. In contrast, rateless codes allow the transmitter to generate an unlimited number of encoded packets, such that the receiver can decode the data after receiving a sufficient number of encoded packets, irrespective of which ones it has received [Shokrollahi2006Raptor]. In addition, rateless codes do not require knowledge of the CSI at the transmitter, and offer greater robustness, reliability and efficiency as compared to fixed-rate codes [Luby2002LT, Erez2012Rateless].

Robustness is a very important issue in a communication network, especially for DSA networks. The network should continue to function even when some of the communication nodes are destroyed or turned off. This means that nodes in the network could be able to work in the peer-to-peer (P2P) or device-to-device (D2D) mode and each node in the network could collaborate with other nodes in a distributed fashion. Therefore, after characterizing the optimal resource allocation and optimal cooperative route for one source-destination pair, we will investigate distributed routing and network scheduling algorithms, and extend it to multiple source-destination pairs. The introduced algorithm will be distributed in the sense that there is no centralized controller that has to have all information about the whole network. When designing distributed algorithms, the objective in this project becomes designing the distributed algorithm in a systematic way. In general, distributed algorithms can be identified through designing a routing metric by experience. Even though a good routing metric yields a reasonable distributed algorithm in certain scenarios, it is far from systematic. Throughout this project, our attention focuses on designing the distributed algorithms systematically, that is, designing the distributed algorithm based on the decomposition of the optimal solution from the centralized problem.

It is important to note that five USRP N210s were borrowed from AFRL to perform the hardware demonstration at the end of this project. Two demonstrations were done at Technical Interchange Meetings (TIM) in June 2015 and May 2016. More specifically, cooperative routing using rateless codes (Raptor Codes) in a five-node DSA network was demonstrated and the performance gain of the hardware demonstration was shown to be in strong agreement with theoretical results.

The project was organized around four interconnected research thrusts:

1) Thrust 1: spectrum sensing for dynamic spectrum access networks;
2) Thrust 2: cooperative routing and resource allocation based on rateless coding for dynamic spectrum access networks;
3) Thrust 3: distributed network resource management for rateless coding-based cooperative dynamic spectrum access networks;
4) Thrust 4: USRP demo using different waveforms, modulation schemes, and multi-access strategies.

In the following sections, we describe the Methods, Assumptions, Procedures, Results and Discussions for each of the aforementioned contributions.

3.0 METHODS, ASSUMPTIONS, AND PROCEDURES

The project can be summarized into four interconnected research thrusts: Thrust 1: spectrum sensing for dynamic spectrum access networks; Thrust 2: cooperative routing and resource allocation based on rateless coding for dynamic spectrum access networks; Thrust 3: distributed network resource management for rateless coding-based cooperative dynamic spectrum access networks; and Thrust 4: USRP demo using different waveforms, modulation schemes, and multi-access strategies.

The following technologies are adopted in the project to advance the objective in each thrust.

Mutual Information Accumulation/Combination Versus Energy Accumulation

In the traditional automatic repeat request (ARQ) transmission, if a data packet is corrupted and cannot be decoded error free at the receiver, the same packet will be requested to be retransmitted. All the previous receptions of the packet will be discarded and this procedure will repeat until the packet is received error free. Since each reception of the packet contains information about the original packet even when it is not decoded error free, it is much more efficient for the receiver to keep the received copy instead of throwing it away. This is the main motivation of hybrid ARQ. There are two classes of hybrid ARQ: chase combining and incremental redundancy.

- ***Chase combining***: every retransmission contains the same information. The receiver uses maximum-ratio combining to combine the received data. Because all transmissions are identical, chase combining can be seen as additional repetition coding. One could think of every retransmission as adding extra energy to the received transmission. Therefore, this mode can also be regarded as energy accumulation.

- ***Incremental redundancy***: every retransmission contains different information than the previous one. Multiple sets of coded bits are generated, each representing the same set of information bits. The retransmission typically uses a different set of coded bits than the previous transmission, with different redundancy versions generated by puncturing the output of the encoder. Therefore, at every retransmission the receiver gains extra information. This mode can also be regarded as mutual information accumulation/combination.

The difference between energy accumulation and mutual information accumulation/ combination is most easily understood by considering binary signaling over a pair of independent erasure channels. Two cooperating transmitters wish to transmit a common message to a single destination. If the erasure probabilities are both p_e, and both transmitters use the same code, then each symbol will be erased with probability p_e^2. Therefore, $1 - p_e^2$ novel parity symbols are received, on average, per transmission. If, instead, the two transmitters use different codes, on average $2(1 - p_e)$ novel parity symbols (which exceeds $1 - p_e^2$) are received per transmission. The latter is mutual-information accumulation/combination, while the former is an example of energy accumulation. From this simple example, it is obvious that mutual information accumulation/combination is strictly better than energy accumulation.

Network Resource Allocation under Mutual Information Accumulation/Combination

When the nodes in a network are equipped with mutual information accumulation/combination, the cooperative communication problem becomes a "***routing***" problem, i.e., identifying which of the available nodes should participate in the transmission and what system resources (time, energy, and spectral bandwidth) should be allocated to each. It is clear that the physical/medium-access-control layer technique employed strongly influences the optimum route.

There has been little prior work investigating routing in networks consisting of nodes using mutual information accumulation/combination. Mutual information accumulation/combination is investigated in [Molisch2007Performance], but the analysis therein assumes network "flooding", i.e., all nodes transmit all the time; this is not an optimum use of energy. In [Zhao2005Practical] a heuristic algorithm for relaying information with chase combining hybrid ARQ *over time* is derived. In contrast to the technique we are going investigate in the proposal, [Zhao2005Practical] assumes that when relay nodes transmit simultaneously, they send out the same signal.

When considering the general task of optimizing route and resource allocations for a communication network with arbitrary attenuation between nodes, our strategy is to introduce first the idea of "transmission order" as illustrated in [Draper2011Cooperative]. In general, "transmission order" is the order in which the nodes are allowed to come on-line as transmitters. We can think of the transmission order as the route used by the cooperative scheme. Since a node cannot transmit until it has decoded the message, a node's position in the transmission order puts constraints on the resources allocated to transmitters prior to it in the order. We then iterate between two sub-problems:

1) First, for the given transmission order, we determine the optimum transmission parameters. This resource allocation problem turns out to be a linear program (LP).
2) Second, based on the solution of the LP we revise the transmission order.

Distributed Network Resource Allocation for Robustness

Robustness is a very important issue in a communication network, especially for aerial layer networks. The network should continue to function even when some of the communication nodes are destroyed or turned off. This means that nodes in the network could be able to work in the P2P or D2D mode and each node in the network could collaborate with other nodes in a distributed fashion. Therefore, after characterizing the optimal resource allocation and optimal cooperative route for one source-destination pair, we will investigate distributed routing and network scheduling algorithms, and extend it to multiple source-destination pairs. The introduced algorithm will be distributed in the sense that there is no centralized controller that has to have all information about the whole network.

When designing distributed algorithms, the objective in this proposal is to design the distributed algorithm in a systematic way. In general, distributed algorithms can be identified through designing a routing metric by experience. Even though a good routing metric yields a reasonable distributed algorithm in certain scenarios, it is far from systematic. Throughout this project, our attention focuses on designing the distributed algorithms systematically, that is, designing the distributed algorithm based on the decomposition of the optimal solution from the centralized problem.

3.1 Spectrum Sensing for Dynamic Spectrum Access Networks

A sensing-based spectrum sharing (SBSS) system [Kang2009Sensing] enables SUs to adapt their transmit power according to their detection of the PUs' status as well as the channel conditions. Compared with the traditional spectrum sharing, SBSS is more flexible and dynamic, allocate system resources to maximize overall system throughput.

3.1.1 The protection of PUs and the sensing throughput trade-off in SBSS

There are two key issues in SBSS system: the protection of PUs and the sensing-throughput trade-off. To protect the PU, an interference power constraint or interference temperature constraint is imposed on SUs in spectrum underlay, while in spectrum overlay, a high detection probability is required in order to maintain PUs' spectrum priority. Therefore, interference power constraints are considered in underlay systems and miss detection constraints are considered in overlay systems. Neither of these constraints can directly measure the Quality-of-Service (QoS) at which cellular links' performance is affected by D2D users. As a result, a rate loss constraint (RLC) is introduced in [Kang2010Optimal] as a new metric which can be directly related to PUs' QoS. This new criterion is shown to provide improved capacity performance over conventional criteria. We adopt a rate loss constraint in our SBSS system.

Another issue in SBSS systems is the sensing-throughput trade-off which is the balance between the protection of PU's performance and the maximization of SUs' throughput. The sensing module should select the best spectrum resource to sense and optimize the sensing time in order to maximize SUs' throughput.

In [Liang2008Sensing] and [Pei2009How], the sensing throughput trade-off in spectrum overlay under the detection probability constraint is investigated. In [Hamdi2009Power], an algorithm to find the optimal sensing time and power allocation for spectrum overlay using interference power constraint is introduced. In [Stotas2011Optimal], the problem of optimizing sensing time and power allocation in SBSS cognitive radio networks under an interference power constraint is studied. In [Shi2012Joint], an optimal power and sub-carrier allocation strategy to maximize SUs' throughput subject to SUs' QoS constraint as well as PU's RLC constraint is introduced for multi-carrier systems.

3.1.2 System model for SBSS

The SBSS system consists of four communication nodes: primary user transmitter (PUT), primary user receiver (PUR), secondary user transmitter (SUT), and secondary user receiver (SUR), as shown in Fig. 1. As in most wireless systems, a frame-based scheme is employed in the SBSS system where the frame structure consists of a sensing slot τ and a data transmission slot T $-\ \tau$. During the sensing slot, energy detection is adopted at the SUT to detect whether the jth sub-carrier is occupied by a PU. The two hypotheses of spectrum sensing can be summarized as:

$$H_0(j): y(m) = z(m) \tag{1}$$

$$H_1(j): y(m) = h_{pst}^{j} x(j,m) + z(m) \tag{2}$$

where h_{pst}^{j} is the channel coefficient between PUT and SUT, $x(j,m)$ is the mth sample of the transmitted signal in the jth sub-carrier, and $z(m)$ is the mth sample of the noise. Denoting the transmit power of PU as P_p, we assume that both the received signal and noise are zero-mean circularly symmetric complex gaussian with variance $\sigma_x^2 = g_{pst}^{j} P_p$ and $\sigma_n^2 = \eta$, respectively. The test statistic for an energy detector is given by

$$T(y) = \frac{1}{f_s T} \sum_{m=1}^{f_s \tau} |y(m)|^2 \tag{3}$$

where f_s is the sampling frequency. The false alarm probability and detection probability in the jth sub-carrier can be written as

$$P_f^j(\varepsilon,\tau) = Pr(T(y) > \varepsilon|H_0) = Q\left(\left(\frac{\epsilon}{\sigma_n^2} - 1\right)\sqrt{\tau f_s}\right) \quad (4)$$

$$P_d^j(\varepsilon,\tau) = Pr(T(y) > \varepsilon|H_1) = Q\left(\left(\frac{\epsilon}{\sigma_n^2} - \gamma^j - 1\right)\frac{\sqrt{\tau f_s}}{\gamma^j + 1}\right) \quad (5)$$

where γ^j is the ratio between power of PU's signals received at SU and noise, $Q(\cdot)$, is the complementary distribution function of the standard Gaussian. To simplify the analysis in the following, the sensing threshold is fixed as $\epsilon = (1 + \gamma^j/2)\sigma_n^2$, which ensures that $P_d \geq P_f$.

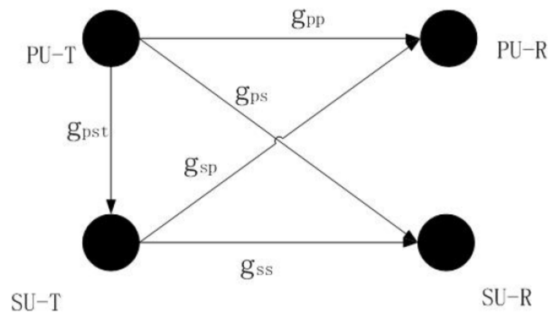

Figure 1: The SBSS system model.

Let $P(H_0)$ denote the probability that PU is idle and $P(H_1)$ denote the probability that PU is busy. If SUT senses PU idle in sub-carrier j, it will transmit at a power level of P_0^j; otherwise, it will transmit at a power level of P_1^j. Let $g_{pp}^j, g_{ps}^j, g_{sp}^j, g_{ss}^j$ represent the channel gains of the jth sub-carrier between PUT and PUR, PUT and SUR, SUT and PUR, SUT and SUR, respectively. Based on PU's activity and SU's sensing results, the throughput of SU can be computed according to the following four scenarios:

1) Scenario 1: SU successfully detects that PU is idle. The probability of this case is $\alpha_0^j = P(H_0)(1 - P_f^j(\tau))$, SU's achievable rate can be expressed as $r_{00}^j = \log_2(1 + P_0^j g_{ss}^j/\eta)$.
2) Scenario 2: SU makes a false alarm. The probability of this case is $\alpha_1^j = P(H_0)P_f^j(\tau)$. SU's achievable throughput can be expressed as $r_{01}^j = \log_2(1 + P_1^j g_{ss}^j/\eta)$
3) Scenario 3: SU fails to detect PU's presence. The probability of this case is $\beta_0^j = P(H_1)(1 - P_d^j(\tau))$. SU's achievable rate can be expressed as $r_{10}^j = \log_2(1 + P_0^j g_{ss}^j/(\eta + P_p^j g_{ps}^j))$.
4) Scenario 4: SU successfully detects PU's presence. The probability of this case is $\beta_1^j = P(H_1)P_d^j(\tau)$. SU's achievable rate can be expressed as $r_{11}^j = \log_2(1 + P_1^j g_{ss}^j/(\eta + P_p^j g_{ps}^j))$

3.1.3 Power Allocation and Sensing Time Optimization Algorithm

In this section, we study the optimal sensing time and power allocation strategy for SBSS networks with PU's RLC. Specifically, in the single-carrier case, we will characterize the optimal system operation and compare the performance (SU's optimal throughput and optimal sensing time) of SBSS with that of a spectrum overlay network. In the multi-carrier case, we will introduce an efficient algorithm to find the optimal sensing time and power allocation.

As the first step, we focus on the single-carrier model where the channel index j is omitted. In this scenario, the SU's average throughput during each frame can be written as:

$$f(\tau, P_0, P_1) = \frac{T-\tau}{T}[\alpha_0 r_{00} + \beta_0 r_{10} + \alpha_1 r_{01} + \beta_1 r_{11}] \tag{6}$$

where r_{00}, r_{01}, r_{10}, r_{11} are SU's achievable rate when SU successfully detects that PU is idle, SU makes a false alarm, SU fails to detect PU's presence, and SU successfully detects PU's presence, respectively.

Denoting δ as the percentage of rate loss that PU can tolerate and $\mathrm{C} = \mathrm{T}\log_2(1 + (g_{pp}P_p)/\eta)$ as PU's data rate without SU's interference, to protect PU's performance, SU should guarantee that PU's average (over sensing results) achievable rate should not be less than $(1-\delta)\mathrm{C}$, which can be expressed in the following equation:

$$\begin{aligned} h_1(\tau, P_0, P_1) = (T-\tau)\left[(1-P_d)\log_2\left(1+\frac{g_{sp}P_0}{\eta + g_{sp}P_0}\right) + P_d\log_2\left(1+\frac{g_{sp}P_0}{\eta+g_{sp}P_1}\right)\right] \\ +\frac{\tau}{T}C - (1-\delta)C \geq 0 \end{aligned} \tag{7}$$

In order to meet the power budget requirement at the SU, an average power constraint (over all sensing results) should be considered, which can be written as:

$$h_2(\tau, P_0, P_1) = P_{tot} - \frac{T-\tau}{T}[(\alpha_0+\beta_0)P_0 + (\alpha_1+\beta_1)P_1] \geq 0 \tag{8}$$

where P_{tot} is SU's average power budget.

Accordingly, in the single-carrier SBSS system, to maximize SU's throughput under PU's rate loss constraint and SU's power constraint, an optimization problem OP1 can be formulated in the following:

$$\max_{\{\tau, P_0, P_1\}} f(\tau, P_0, P_1) \tag{9}$$

$$\mathrm{s.t.}: h_1(\tau, P_0, P_1) \geq 0, h_2(\tau, P_0, P_1) \geq 0, P_0 \geq 0, P_1 \geq 0, T \geq \tau \geq 0$$

In the multi-carrier case, let J denote the total number of sub-carriers in the system. Furthermore, we assume that both PU and SU can occupy several channels concurrently based on the channel conditions and sensing results. Accordingly, SU's throughput optimization problem in multi-carrier case under PU's rate loss constraint and SU's transmission power constraint can be formulated as:

$$\max_{\{\tau,\boldsymbol{P_0},\boldsymbol{P_1}\}} f(\tau,\boldsymbol{P_0},\boldsymbol{P_1}) = \frac{T-\tau}{T}\sum_{j=1}^{J}\left[\alpha_0^j r_{00}^j + \beta_0^j r_{10}^j + \alpha_1^j r_{01}^j + \beta_1^j r_{11}^j\right] \tag{10}$$

$$\text{s.t.}: g_1(\tau,\boldsymbol{P_0},\boldsymbol{P_1}) \geq 0, g_2(\tau,\boldsymbol{P_0},\boldsymbol{P_1}) \geq 0$$

where $\boldsymbol{P_0} = \left(P_0^1, P_0^2, \dots, P_0^J\right), \boldsymbol{P_1} = \left(P_1^1, P_1^2, \dots, P_1^J\right)$. $g_1(\tau,\boldsymbol{P_0},\boldsymbol{P_1})$ represents PU's RLC and $g_2(\tau,\boldsymbol{P_0},\boldsymbol{P_1})$ represents SU's average (over sensing results) power constraint.

The solution to find the optimal sensing time and power allocation in single-carrier case is summarized in the following algorithm:

Algorithm 1: Find optimal sensing time and power allocation in single-carrier SBSS

Input: System parameters: T, δ, $P(H_0)$, η, P_{tot}, f_s, $\{g_{ss}, g_{sp}, g_{ps}, g_{pp}, P_p\}$;
Output: Optimal sensing time τ and Power allocation P_0, P_1;

for $\tau \leftarrow 0$ ***to*** T **do**
    calculate S_1 by (10);
    calculate S_2 by (13);
    calculate S_3 by (14);
    find the optimal power under τ, $(P_0(\tau), P_1(\tau))$, by (15);
$\tau^* = \arg\max_{T \geq \tau \geq 0} f\left(\tau, P_0(\tau), P_1(\tau)\right)$;
$(P_0^*, P_1^*) = (P_0(\tau^*), P_1(\tau^*))$;
return $\tau^*, (P_0^*, P_1^*)$.

The solution to find the optimal sensing time and power allocation in multi-carrier case is summarized in the following algorithm:

Algorithm 2: Find optimal sensing time and power allocation in multi-carrier SBSS

Input: System parameters: T, δ, $P(H_0)$, η, P_{tot}, f_s, $\{g_{ss}^j, g_{sp}^j, g_{ps}^j, g_{pp}^j, P_p^j, j = 1, ..., J\}$

Output: Optimal sensing time τ^* and Power allocation $\mathbf{P_0}^*, \mathbf{P_1}^*$

Initialization:
$\mathbf{P_0}(0), \mathbf{P_1}(0), 0 < \nu \ll 1, \theta \in (0,1), \eta > 1,\ k \leftarrow 1,$
c(0)$>$ 0, $\beta(0) \leftarrow \nu + 1$;

for $\tau \leftarrow 0$ ***to*** T **do**
    while $\beta(k-1) > \nu$ **do**
        Start from $(\mathbf{P_0}(k-1), \mathbf{P_1}(k-1))$, solve the unconstrained optimization problem (18) using BFGS method and get the minimal point as $(\mathbf{P_0}(k), \mathbf{P_1}(k))$;
        if $\beta(k) > \theta\beta(k-1)$ **then**
            $c(k+1) \leftarrow \eta c(k)$;
        else
            c(k+1) $\leftarrow$ c(k);
        update μ_j by (19);
        $k \leftarrow k + 1$;
    $(\mathbf{P_0}^*(\tau), \mathbf{P_1}^*(\tau)) \leftarrow (\mathbf{P_0}(k), \mathbf{P_1}(k))$;

$\tau^* \leftarrow \arg\max_{T \geq \tau \geq 0} f(\tau, \mathbf{P_0}^*(\tau), \mathbf{P_1}^*(\tau))$;
$(\mathbf{P_0}^*, \mathbf{P_1}^*) \leftarrow (\mathbf{P_0}^*(\tau^*), \mathbf{P_1}^*(\tau^*))$;
return $\tau^*, \mathbf{P_0}^*, \mathbf{P_1}^*$;

3.2 Rateless Coding based Cooperative Dynamic Spectrum Access Networks

As introduced in the former sections, mutual-information accumulation is an enhanced technique to increase the performance of the dynamic spectrum access network which can be realized through rateless codes. Rateless codes allow the transmitter to generate an unlimited number of encoded packets, such that the receiver can decode the data after receiving a sufficient number of encoded packets, irrespective of which ones it has received [Shokrollahi2006Raptor]. In addition, rateless codes do not require knowledge of the channel state information (CSI) at the transmitter, and offer robustness, reliability and efficiency as compared to fixed-rate codes [Luby2002LT, Erez2012Rateless].

3.2.1 Improving the throughput of CRN/DSA with mutual-information accumulation

In DSA networks, unlicensed users or secondary users (SUs) periodically sense the spectrum to detect any licensed or primary user (PU) activity before transmission. A SU needs to maximize its opportunistic transmissions while being "transparent" to PU's activities. In practice, a primary receiver (PR) may fail to decode the packets from a primary transmitter (PT) due to the interference of SUs or "too weak" channel condition. To increase SU transmission opportunities and increase PU throughput, the SU can relay PU packets that are unsuccessfully received at the PR. This would help free up PU's queue faster so SU can have more channel access [Simeone2007Stable, Zhang2013On, Chen2015Optimal]. To enhance the performance of PUs, mutual-information accumulation technique can be used at the PR.

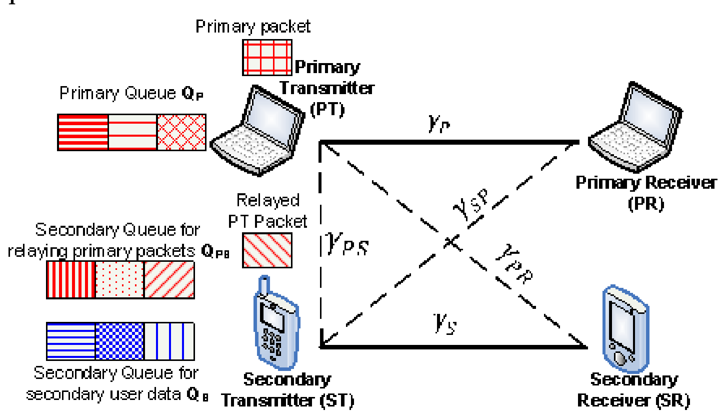

Figure 2: A general system model that a pair of SUs co-exit with a pair of PUs.

Fig. 2 shows a CRN where a pair of SUs coexit with a pair of PUs [Devroye2006Achievable]. ST senses PT's activity at the beginning of the time slot, if detected idle, ST will transmit a packet, provided it has at least one in its queue. PT and ST are equipped with queues of infinite length, with ST having two queues: one holding its own packets, and the other holding PT packets that were unsuccessfully received by PR.

Independent and stationary traffic arrival processes are considered for primary and secondary queues, with arrival rates λ_i, and departure rates μ_i packets/sec, where i reads "P" for Q_P (holding

PT packets), “S” for Q_S (holding ST own packets), and “PS”, “SP” for Q_{PS} (holding PT packets to be relayed by ST). PT transmits with normalized power $P_P = 1$, while ST selects its transmission power $P_S \leq 1$. A packet is successfully received at the intended destination if the SNR is above a threshold β_i, where i reads “P” for primary, and “S” for secondary. The probability of an outage event is

$$P_{\text{out},i} = P[\gamma_i \,|h_i(t)|^2\, P_i < \beta_i] = 1 - e^{-\frac{\beta_i}{\gamma_i P_i}} \tag{11}$$

Due to fading and path loss, ST may misdetect PT’s transmission with probability p_m, causing undesirable interference to the primary link. Also ST might detect the idle slot as busy with a false alarm probability p_f. The departure rate $X_P(t)$ of the primary transmitter, can be defined as the number of primary packets that are successfully received at either PR or ST at time t. Then

$$\begin{aligned}\mathbf{E}[X_P(t)] &= \mathbf{E}\left\{\mathbf{1}\left\{O_P(t) \cup O_P^I(t)\right\}\right\} = \mu_P^r \\ &= (1-p_m)\left(e^{-\frac{\beta_P}{\gamma_P}} + e^{-\frac{\beta_P}{\gamma_{PS}}} - e^{(\frac{-\beta_P}{\gamma_P} - \frac{\beta_P}{\gamma_{PS}})}\right) + p_m\left(\frac{\gamma_P e^{-\frac{\beta_P}{\gamma_P}}}{\gamma_P + \beta_P \gamma_{SP} P_S}\right).\end{aligned} \tag{12}$$

$O_P(t)$ and $O_P^I(t)$ denote the events that PT successfully transmits without interference from ST and under ST interference, respectively.

The departure rate $X_S(t)$ of the secondary queue Q_S is defined as the number of secondary packets that are successfully transmitted to the intended SR at time t, and

$$\begin{aligned}\mathbf{E}[X_S(t)] &= \mathbf{E}\left\{\mathbf{1}\left\{\left(A_S(t) \cap O_S(t)\right) \cup \left(A_S^I(t) \cap O_S^I(t)\right)\right\}\right\} = \mu_S(P_S, \epsilon) \\ &= (1-p_f)\left(1 - \frac{\lambda_P}{\mu_P^r}\right) e^{-\frac{\beta_S}{P_S \gamma_S}}(1-\epsilon) + p_m\left(\frac{\lambda_P}{\mu_P^r}\right)(1-\epsilon)\frac{P_S \gamma_S e^{\frac{-\beta_S}{P_S \gamma_S}}}{P_S \gamma_S + \beta_S \gamma_{PR}}.\end{aligned} \tag{13}$$

where $A_S(t)$ and $A_S^I(t)$ denote the events that slot t is available for transmission by ST when correctly sensed as idle when misdetected as idle, respectively. $O_S(t)$ and $O_S^I(t)$ denote the events of successful transmission by ST under no interference from PT and under PT interference, respectively. ϵ is the probability that ST transmits PT packet when the slot is sensed idle [Elazzouni2015Fullduplex].

Similarly, $X_{SP}(t)$ is defined as the number of successful reception by PR from ST without interference from PT and under PT interference, respectively. Then

$$\mathbf{E}[X_{SP}(t)] = \mathbf{E}\left\{\mathbf{1}\left\{\left(A_s(t)\cap O_{SP}(t)\right)\cup\left(A_s^I(t)\cap O_{SP}^I(t)\right)\right\}\right\} = \mu_{SP}(P_S,\epsilon)$$
$$= (1-p_f)\left(1-\frac{\lambda_P}{\mu_P^r}\right)e^{-\frac{\beta_P}{\gamma_{SP}P_S}}\cdot\epsilon + p_m\left(\frac{\lambda_P}{\mu_P^r}\right)\frac{P_S\gamma_{SP}e^{-\frac{\beta_P}{\gamma_{SP}P_S}}}{P_S\gamma_{SP}+\beta_P\gamma_P}\cdot\epsilon \tag{14}$$

where $O_{SP}(t)$ and $O_{SP}^I(t)$ denote the events of successful reception by PR from ST with/without interference from PT, respectively. The arrival rate of Q_{PS} is defined as the number of primary packets that are to be relayed by ST, then the average arrival rate of Q_{PS} can be written as

$$\lambda_{PS} = \frac{\lambda_P}{\mu_P^r}\left(1-e^{\frac{-\beta_P}{\gamma_P}}\right)e^{\frac{-\beta_P}{\gamma_{PS}}}. \tag{15}$$

$\lambda_{PS} < \mu_{SP}(P_S,\epsilon)$ should be guaranteed to keep the stability of the queue $Q_{PS}(t)$, then

$$\epsilon \geq \frac{\frac{\lambda_P}{\mu_P^r}\left(1-e^{-\frac{\beta_P}{\gamma_P}}\right)e^{-\frac{\beta_P}{\gamma_{PS}}}}{(1-p_f)\left(1-\frac{\lambda_P}{\mu_P^r}\right)e^{-\frac{\beta_P}{\gamma_{SP}P_S}} + p_m\left(\frac{\lambda_P}{\mu_P^r}\right)\frac{P_S\gamma_{SP}e^{-\frac{\beta_P}{\gamma_{SP}P_S}}}{P_S\gamma_{SP}+\beta_P\gamma_P}}. \tag{16}$$

The above optimal ϵ to maximize the throughput of the CRN is valid when mutual-information accumulation is not used. When mutual-information accumulation is used, everything remains valid except the probability of $O_{SP}(t)$. In mutual-information accumulation, nodes accumulate information as $C_{i,j}t$ bits/Hz, where $C_{i,j}$ is the channel capacity between nodes i and j, then the probability of $O_{SP}(t)$ can be modified as

$$P[O_{SP}(t_2)] \triangleq k_s(P_S) = w_1\left(e^{-\frac{\beta_P}{\gamma_{SP}P_S}} + \frac{e^{\frac{1}{\gamma_{SP}P_S}+\frac{1}{\gamma_P}}}{\gamma_{SP}P_S}\int_1^{1+\beta_P} e^{-\frac{g(M_1)}{\gamma_{SP}P_S}-\frac{1+\beta_P}{g(M_1)\gamma_P}}\,dg(M_1)\right) + w_2\left(\int_0^{g(\beta_P)}\frac{\gamma_P e^{-\frac{2^{g(\beta_P)-y_1}-1}{\gamma_P}}}{\gamma_P+P_S\gamma_{SP}\left(2^{g(\beta_P)-y_1}-1\right)}f_{Y_1}(y_1)\,dy_1 + \frac{P_S\gamma_{SP}e^{-\frac{2^{g(\beta_P)}-1}{P_S\gamma_{SP}}}}{P_S\gamma_{SP}+\gamma_P\left(2^{g(\beta_P)}-1\right)}\right)$$
$$+ w_3\left(\frac{P_S\gamma_{SP}e^{-\frac{2^{g(\beta_P)}-1}{P_S\gamma_{SP}}}}{P_S\gamma_{SP}+\gamma_P\left(2^{g(\beta_P)}-1\right)} + \int_0^{g(\beta_P)} e^{-\frac{2^{g(\beta_P)-1}-1}{\gamma_P}} f_{Y_1}(y_1)\,dy_1\right) + w_4\left(e^{-\frac{2^{g(\beta_P)}-1}{P_S\gamma_{SP}}} + \int_0^{g(\beta_P)}\frac{\gamma_P e^{-\frac{2^{g(\beta_P)-y_2}-1}{\gamma_P}}}{\gamma_P+P_S\gamma_{SP}\left(2^{g(\beta_P)-y_2}-1\right)}f_{Y_2}(y_2)\,dy_2\right) \tag{17}$$

where

$$M_1 = \gamma_P |h_P(t_1)|^2, \quad M_2 = \frac{\gamma_P |h_P(t_1)|^2}{1 + P_S \gamma_{SP} |h_{SP}(t_1)|^2}, \quad w_1 = \frac{(1-p_m)\left(1-\frac{\lambda_p}{\mu_p^r}\right)(1-p_f)}{p_t}, \quad w_3 = \frac{(1-p_m)\left(\frac{\lambda_p}{\mu_p^r}\right)p_m}{p_t},$$

$$N_1 = P_S \gamma_{SP} |h_{SP}(t_2)|^2, \quad N_2 = \frac{P_S \gamma_{SP} |h_{SP}(t_2)|^2}{1 + \gamma_P |h_P(t_2)|^2}. \quad w_2 = \frac{p_m^2\left(\frac{\lambda_p}{\mu_p^r}\right)}{p_t}, \quad w_4 = \frac{p_m\left(1-\frac{\lambda_p}{\mu_p^r}\right)(1-p_f)}{p_t}. \tag{18}$$

Also, to guarantee the stability of the queue $O_{PS}(t)$, $\epsilon \geq \lambda_{PS}/k_S(P_S)$ should be met. Note that this equation can be solved numerically.

3.2.2 Cooperative Routing for Underlay CRNs using mutual-information accumulation

In CRNs, SUs have to dynamically control their transmit powers so that the interference to PUs is tolerable. Under this constraint, SUs' data link usually suffers from either high error rate with limited transmission range or long end-to-end delay cause by multi-hop transmissions. To address this issue, a cooperative routing strategy among SUs that employs advanced channel coding strategies such as mutual-information accumulation is applied to extend SU networks' coverage [Palanki2004Rateless, Castura2007Rateless]. The objective of the SU is to minimize the end-to-end delay under sum-bandwidth, sum-energy and PU's interference power constraint.

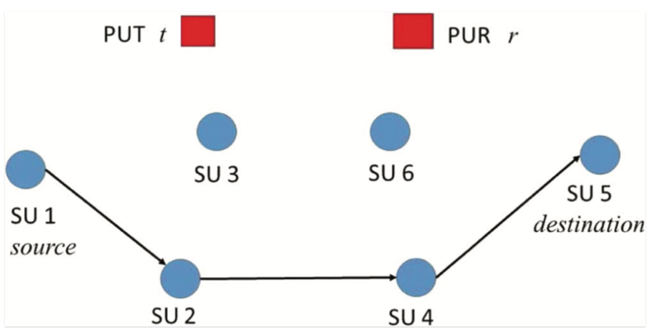

Figure 3: System model of Underlay CRN with a pair of PUs and N SUs.

Fig. 3 shows a underlay CRN containing 1 PU transmitter, 1 PU receiver, 1 SU source, 1 SU destination and $N-2$ SU relays. The spectrum bandwidth of the subband is denoted as W_T, and PU's interference power threshold is I_T. The SU network needs to transmit a data packet with an entropy of B bits from the SU source to SU destination with the help of SU relays. Depending on the routing and resource allocation strategies, all SU nodes may actively help forwarding the packet or keep silent. Let P_S be the transmit power spectral density of SUs. The channel power gain between node i and j is h_{ij}. C_{ij} is the achievable transmission rate per degree of freedom between node i and j

$$C_{i,j} = \log_2\left(1 + \frac{h_{ij} P_S}{\left(N_0 + h_{pj} P_p\right)\Gamma}\right) \frac{\text{bits}}{\text{sec} \cdot \text{Hz}}, \tag{19}$$

where P_P is the transmit power spectral density of PU, Γ is the SNR gap between the channel capacity and a practical modulation and coding scheme.

Let L be the total number of nodes in the transmission order. $\Delta_i = T_i - T_{i-1}$ is the inter-user delay between user i and user i-1. T_i is the time at which user i decodes the message, and Δ_i can be regarded as the length of the ith time slot. For a given route order, the objective of the SU network is to minimize end-to-end transmission delay T_L:

$$\mathbf{OP1}: T_L = \sum_{i=1}^{L} \Delta_i \tag{20}$$

The minimization problem is constrained by the following constraints:

$$\sum_{i=0}^{k-1} \sum_{j=i+1}^{k} A_{ij} C_{ij} \geq B, \quad k = 1, \cdots, L. \tag{21}$$

where A_{ij} denotes the time-bandwidth product assigned to the ith user in the jth time slot. This equation means that the accumulated mutual information should exceed the entropy after L transmissions.

$$\sum_{i=0}^{L-1} \sum_{j=i+1}^{L} A_{ij} P_S \leq E_T \tag{22}$$

this constraint means the total energy consumption for delivering the message throughout the SU network should not exceed the energy budget E_T [Neely2005Dynamic].

$$\sum_{i=0}^{j-1} A_{ij} \leq \Delta_j W_T, \quad j = 1, \cdots, L, \tag{23}$$

this constraint suggests that all the nodes in the SU network share a sum-bandwidth of W_T.

$$\sum_{i=0}^{j-1} A_{ij} h_{ir} P_S / \Delta_j \leq I_T, \quad \Delta_j \neq 0, j = 1, \cdots, L-1, \tag{24}$$

To protect the PU's QoS, SUs should make sure that their total interference powers to the PU receiver should not exceed I_T. h_{ir} is the channel power gain from the ith SU to the PU receiver.

In fact, OP1 is NP-complete, but if the transmission order is determined, then the problem is easy to solve. Let $x^* = [\Delta_1^*, \Delta_2^*, \dots, \Delta_L^*, A_{01}^*, A_{02}^* \dots, A_{0L}^*, A_{12}^*, \dots, A_{(L-1)L}^*]$ be the optimal solution of OP1 for a given route/transmission order. Denote the corresponding optimal end-to-end delay as

$$T_L^* = \sum_{i=1}^{L} \Delta_i^* \tag{25}$$

Then the following theorem holds:

- Theorem 1: if $\Delta_i^* = 0$, let T_L^{**} be the optimal end-to-end delay of the "swapped" route/ transmission order

  $$[0, \cdots, i-2, i, i-1, i+1, \cdots, L] \quad \text{if } i \le L-1$$
  $$[0, \cdots, L-2, L] \quad \text{if } i = L.$$

  then $T_L^{**} \le T_L^*$.

- Theorem 2: If user i's transmission time is 0, let T_L^{**} denote the optimal end-to-end delay of the "deleted" transmission order:

  $$[0, \cdots, i-1, i+1, \cdots, L] \text{ if } i \le L-1$$

  then $T_L^{**} \le T_L^*$.

From the above two theorems, we know that for any route/transmission order, the "sweeping" and "deleting" operation can be used to obtain a better route/transmission order.

Algorithm 1 shows the detailed iterative route optimization and resource allocation algorithm. In every repeat, the OP1 problem is solved, the iteration terminates once an order with $\Delta_i > 0$, and $t_i > 0$ for all i is obtained.

Algorithm 1: Centralized cooperative routing and resource allocation algorithm

Input: System parameters: $P_s, P_p, N_0, \alpha, I_T, E_T, \{h_{ij} | 1 \leq i, j \leq N\}, \{h_{ir} | 1 \leq i \leq N-1\}, \{h_{pi} | 2 \leq i \leq N\}$;

Output: Route from the SU source to the SU destination and the corresponding resource allocation A_{ij};

Initialization: Apply Dijkstra algorithm to find the optimal path from the source to the destination with the minimal interference to the PU receiver; take this minimal interference path as the initial transmission order;

repeat

  solve the linear program **OP1** to get the resource allocation solution for current transmission order;

  (Based on Theorem 1 swap the transmission order);

  if $\Delta_i = 0$ *and* $\Delta_{i-1} \neq 0, i = 1, \ldots, L$ **then**

    swap the positions of the two nodes in the order;

  if $\Delta_L = 0$ **then**

    drop node $L-1$ from the order;

  (Based on Theorem 2 delete the silent node);

  if $t_i = 0$ **then**

    drop node i from the order;

until *An order with* $\Delta_i > 0$ *and* $t_i > 0$ *for all* i *is obtained*;

3.3 Distribute Resource Allocation

Centrally determining resource allocation for all candidate transmission nodes in a large-scale network, if even possible, is an exceedingly expensive operation. A potential solution is to perform distributed resource allocation in which the resource allocation is determined locally. Compared with the centralized resource allocation, the distributed scheme is a quite cost-efficient, flexible, and robust, and is widely used in many research fields such as massive machine type communication (MTC) and cooperative routing in multi-hop cognitive radio networks (CRNs).

3.3.1 Cooperative Retransmission for massive MTC

In massive MTC networks, multiple machine type devices (MTDs) need to transmit packets to their base stations (BS) [Andrews2014What]. The wireless connection between the MTD and the BS is unreliable, however, due to the interference caused by uncoordinated access of other MTDs [Dhillon2015Wide]. Worse yet is that the probability that the retransmission from the outage source MTD will fail again due to the spatiotemporally correlated interference is high [Ganti2012Spatial, Nigam2015Spatiotemporal, Haenggi2013Diversity]. It is impossible for the BS to centrally perform a perfect schedule to all MTDs to avoid such interference. A potential solution is to apply a distributed location-based cooperative strategy to improve the performance of massive MTC networks.

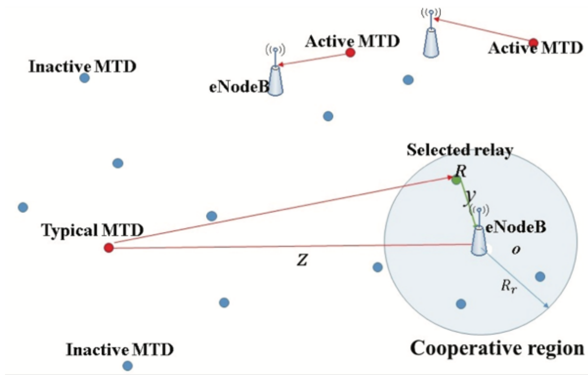

Figure 4: System model of the distributed cooperative retransmission strategy.

Fig. 4 shows the system model of the cooperative strategy. In the cooperative strategy, an inactive MTD is selected as a relay to forward the packets of the outage source MTD in the first transmission. The relay MTD is selected based on the following two requirements:

1) The inactive relay MTD has successfully decoded the packet in the first transmission;

2) The relay MTD is located within a circular area A_r around the BS with a radius of R_r to make sure the relayed packet can be decoded by the BS with a high probability.

Assume the locations MTDs are modeled as a homogeneous Poisson point process (HPPP) ϕ with a density of λ [Dhillon2014Fundamentals]. MTDs transmit collected data to BS with probability p. The typical BS fails to decode a packet if the received SIR is less than a threshold T, and all MTDs transmit with the same power P_t. Therefore, the received power at the typical BS from a MTD at a distance of z is $P_r = P_t G_{s,d,1} z^{-\alpha}$, where $G_{s,d,1} \sim \exp(1)$ is the small scale fading gain between the typical MTD s and the typical BS d during the first transmission.

Under the designed cooperative strategy, the typical BS is outage if: 1) there is a potential relay selected but the typical BS fails to decode the packet after the retransmission from the potential relay; or 2) there is no potential relay and the typical BS fails to decode the packet after the retransmission from the typical MTD. Thus, the outage probability of the designed cooperative strategy can be expressed as

$$P^{co} = P(B) - P(A \cap B \cap E) - P(A^c \cap B \cap F). \qquad (26)$$

In the equation, A is the event that there is at least one potential relay. B denotes the event that the first transmission from the typical MTD fails. E means the transmission from the selected relay succeeds, and F indicates that the retransmission from the typical MTD succeeds. A^c denotes the complement of A and $P(\mathrm{B}) = 1 - e^{-c1}$ is the outage probability of the first transmission. After the derivation, the formulation of $P(\mathrm{A} \cap \mathrm{B} \cap \mathrm{E})$ and $P(A^c \cap \mathrm{B} \cap \mathrm{F})$ can be listed as follows

$$P(\mathrm{A} \cap \mathrm{B} \cap \mathrm{E}) = \int_0^{R_r} P_{re}^s(y) 2y/R_r^2 dy \tag{27}$$

$$P(A^c \cap \mathrm{B} \cap \mathrm{F}) = e^{-c_1} - e^{-a-2c_1+p(1-\sigma)c_1} + \sum_{k=1}^{\infty}\sum_{j=1}^{k+1} \frac{(-1)^j e^{-a} a^k (k+1)}{j!\,(k+1-j)!} e^{-pg(j+1)\lambda} \tag{28}$$

where

$$P_{re}^s(y) = \sum_{k=1}^{\infty}\sum_{j=1}^{k} \frac{e^{-a}a^k}{k!} C_k^j (g_2(j+1,y) - g_2(j,y)), \tag{29}$$

Therefore, in a massive MTC network, the outage probability for a typical MTD link under the distributed cooperative strategy can be expressed as

$$\begin{aligned} P^{co} &= 1 - 2e^{-c_1} + e^{-a-2c_1+p(1-\sigma)c_1} - \\ &\sum_{k=1}^{\infty}\sum_{j=1}^{k+1} \frac{(-1)^j e^{-a} a^k (k+1)}{j!(k+1-j)!} e^{-p\lambda(g(j)-(1-p)g(1)-p(g(j+1)-g(j)))} \\ &-\sum_{k=1}^{\infty}\sum_{j=1}^{k} \frac{(-1)^j e^{-a} a^k}{j!(k-j)!} \int_0^{R_r} \frac{2y}{R_r^2} (g_2(j+1,y) - g_2(j,y)) dy \end{aligned} \tag{30}$$

3.3.2 Distributed Cooperative Routing and Resource Allocation in Underlay CRNs

In Section 3.2.2, the cooperative routing for underlay CRNs using mutual-information accumulation is described, but the optimal cooperative routing and resource allocation algorithm is proposed centrally. The operation is inefficient in large-scale network, thus a distributed cooperative routing and resource allocation algorithm is needed to take link achievable rate, link interference to the PU receiver, and mutual-information accumulation into consideration. In fact, distributed algorithms have been studied in [Draper2011Cooperative] and [Urgaonkar2012Optimal], but they do not take the interference from SUs to PUs. Although [Chowdury2011CRP], [Caleffi2012OPERA] and [Chen2012A] consider the interference power constraint of PUs, they cannot be directly used in CRNs with mutual-information accumulation.

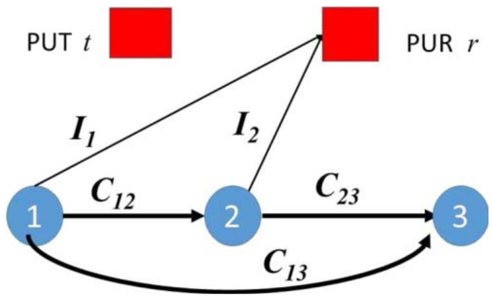

Figure 5: A simple three-node SU network.

Take a simple three-node SU network as an example. As shown in Fig. 5, assume that node 1 and node 2 have already successfully decoded the message while node 3 still needs to receive B_0 bits of mutual information before successfully decoding the message. C_{12} , C_{13} , C_{23} are respectively the link achievable rates among node 1, 2 and 3. I_T is the interference threshold set by the PU receiver and the total bandwidth of the subband is normalized to $W_T = 1$. θ_1 and θ_2 are the spectrum bandwidth allocated to node 1 and node 2. The interference power spectral density of node 1 and node 2 to the PU receiver are thus respectively $I_1 = h_{1r}P_S$, and $I_2 = h_{2r}P_S$, then the optimal spectrum resource allocation can be expressed as

$$(\theta_1^*,\theta_2^*)=\begin{cases} (1,0) & \text{if } I_1 \le I_T, C_{23} \le C_{13}; \\ (0,1) & \text{if } I_2 \le I_T, C_{23} \ge C_{13}; \\ (0,\dfrac{I_T}{I_2}) & \text{if } I_2 \ge I_T, C_{23} \ge \dfrac{I_2 C_{13}}{I_1}, \\ & \text{and } I_1 \ne I_2; \\ (\dfrac{I_T}{I_1},0) & \text{if } I_1 \ge I_T, C_{23} \le \dfrac{I_2 C_{13}}{I_1}, \\ & \text{and } I_1 \ne I_2; \\ & \text{if } I_1 > I_T, I_2 < I_T, \\ (\dfrac{I_T - I_2}{I_1 - I_2}, \dfrac{I_1 - I_T}{I_1 - I_2}) & \text{and } C_{13} > C_{23} > \dfrac{I_2 C_{13}}{I_1}; \\ & \text{if } I_1 < I_T, I_2 > I_T, \\ (\dfrac{I_2 - I_T}{I_2 - I_1}, \dfrac{I_T - I_1}{I_2 - I_1}) & \text{and } C_{13} < C_{23} < \dfrac{I_2 C_{13}}{I_1}; \end{cases} \tag{31}$$

The θ_1^* and θ_2^* can be applied to minimize the end-to-end delay. From the equation, we find the delay-optimal cooperative route for underlay CRNs depends on both the interference condition and the link achievable rate condition; and under some interference and link achievable rate conditions, both node 1 and node 2 have the opportunity to participate in the transmission simultaneously (see the fifth and sixth items).

The above equation is the optimal solution for a three-node network. To extend the result to multiple nodes scenario the problem can be solved by introducing the concept of a virtual node. If there are two nodes, say node 1 and node 2, doing concurrent transmission at the same slot, the two nodes combined can be regarded as a virtual node $\hat{2}$. If a node decodes the packet and determines that a virtual node is transmitting in the network, this node will not transmit concurrently with the virtual node, and within a slot, there are at most two SUs sharing PU's spectrum and transmitting concurrently. Further, for the underlay CRN with M primary pairs, within a slot there are at most $M + 1$ SUs sharing PU's spectrum and transmitting concurrently.

The following algorithm determines the distributed routing and resource allocation algorithm for underlay CRNs with mutual-information accumulation. The computational complexity of this distributed algorithm for each node is $O(1)$, and the overhead of our distributed algorithm can be quite small.

Algorithm 2: Distributed routing and resource allocation algorithm for underlay CRNs with MIA

1 Initialization: (For node i) Estimate its interference power spectral density I_i to the PU receiver; estimate its channel to the destination and calculate C_{iN}; obtain the information of current transmitting node I_{i-1} and $C_{(i-1)N}$ from the header of the data packet it has decoded;

2 calculate θ_1, θ_2 by equation (7);

3 **if** $\theta_1 = 0, \theta_2 > 0$ **then**

4   Set $\theta_1 = 0$ in the control packet and send it out to inform current transmitting node to stop transmitting; set V_flag to be FALSE; add C_{iN}, I_i in the header and start to transmit;

5 **else if** $\theta_1 > 0, \theta_2 > 0$ **then**

6   Set θ_1 in the control packet using the computed value of θ_1 in step 2; send out the control packet; in the header of a data packet, set V_flag to be TRUE; set C_{iN} to be the equivalent achievable rate of the virtual node; set I_i to be I_T; transmit data packet with bandwidth θ_2;

7 **else**

8   node i keeps silent.

3.4 USRP Demo

USRP N210s are used to demonstrate our results. More specifically, we construct a five-node DSA/CRN network and using GNU radio to implement the protocol. Two applications are demonstrated: 1) image file transfer over the SU network, and 2) video file transfer over the SU network.

The GNU radio node design can be found in the following figure.

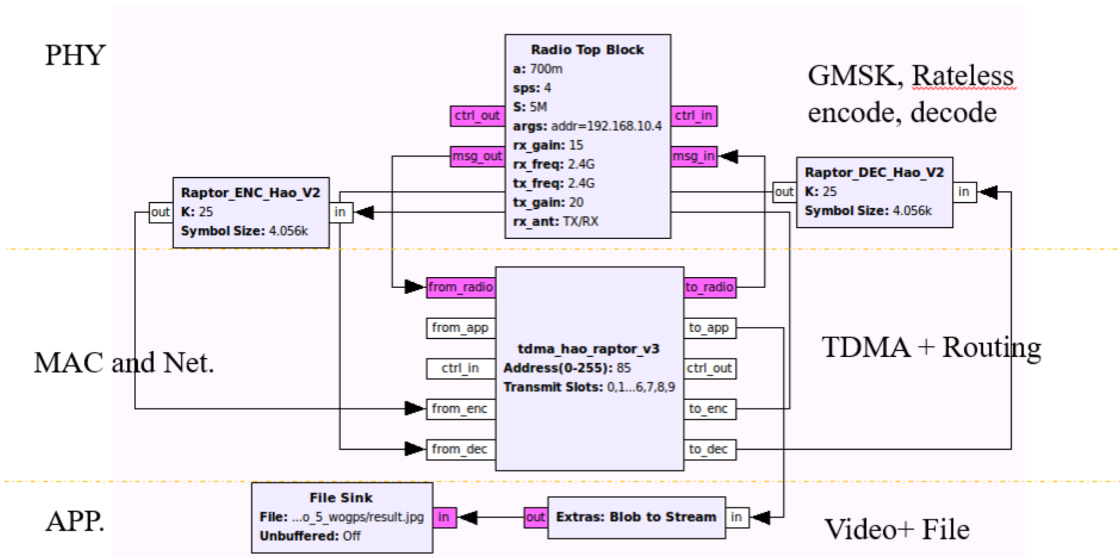

Figure 6: Source Node Design (GNU Radio)

The GNU physical layer design can be found in the following figure.

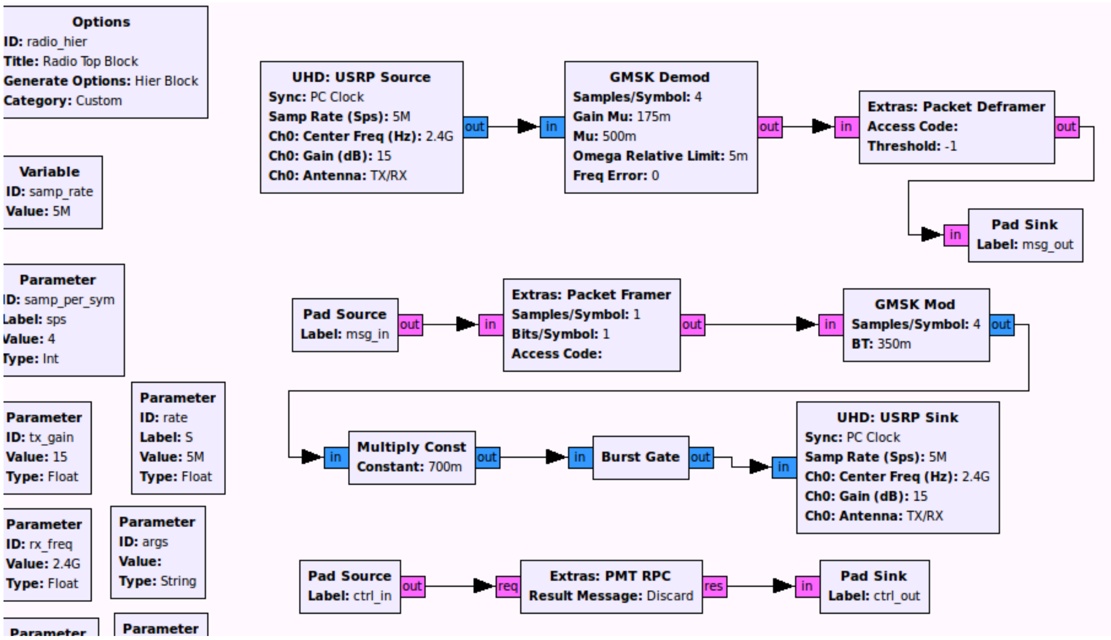

Figure 7: PHY Layer Design (GNU Radio)

4.0 RESULTS AND DISCUSSION

4.1 Spectrum Sensing for Dynamic Spectrum Access Networks

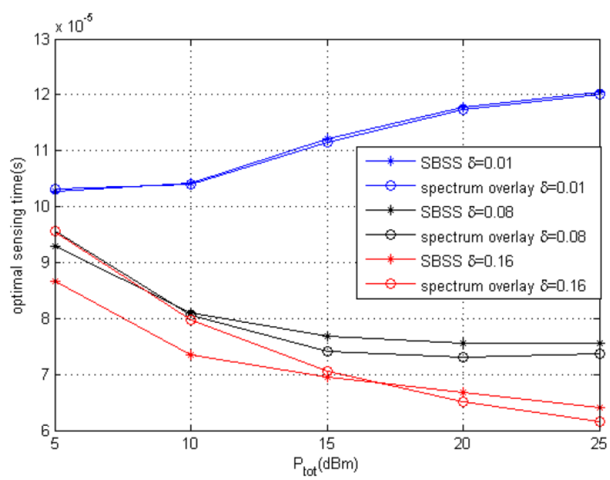

Figure 8: Optimal sensing time versus total transmit power of SU.

Fig. 8 shows the relationship between SU's optimal sensing time and SU's total transmit power. Each point in the figure is the average results of 5000 simulation runs and $P(H_0) = 0.7$. We can see that when PU has stringent rate loss constraint, as SU's power budget increases, SU will spend more time on sensing. However, if PU can tolerant much larger rate loss, as SU's power budget increases, SU's optimal sensing time decreases. This difference is caused by the exchange of the dominant constraint of the system. Another interesting finding is that when SU's power budget is low, the optimal sensing time of SBSS will be smaller than that of spectrum overlay. But as SU's power budget increases, SU's optimal sensing time in SBSS will be larger than that of spectrum overlay.

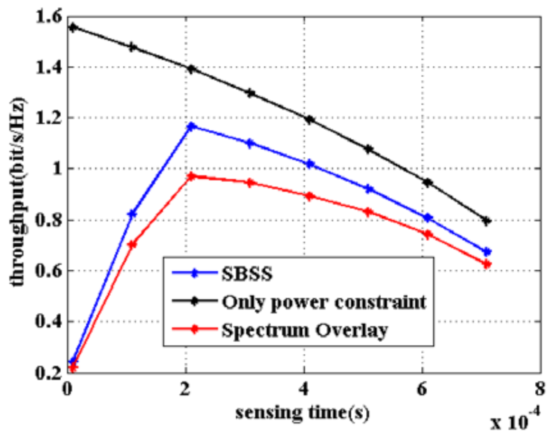

Figure 9: SU's throughput versus SU's sensing time

Fig. 9 compares the performance of SBSS and spectrum overlay in multi-carrier case under different sensing times. The black line represent the throughput of cognitive system with only power constraint. The total number of carriers is set as 30, PU's power is 25 dBm and SU's total power budget is 20 dBm (these two parameters are set as 30 times of corresponding values in the single-carrier case). PU's rate loss δ is set as 0.1. From this picture, we can see that in multi-carrier case, SBSS can improve the spectrum efficiency one step further compared to the corresponding single-carrier case, specifically, under the optimal sensing time (0.2ms), SBSS will achieve 15.2% more spectrum efficiency than spectrum overlay.

4.2 Rateless Coding based Cooperative Dynamic Spectrum Access Networks

4.2.1 Improving the throughput of CRN with mutual-information accumulation

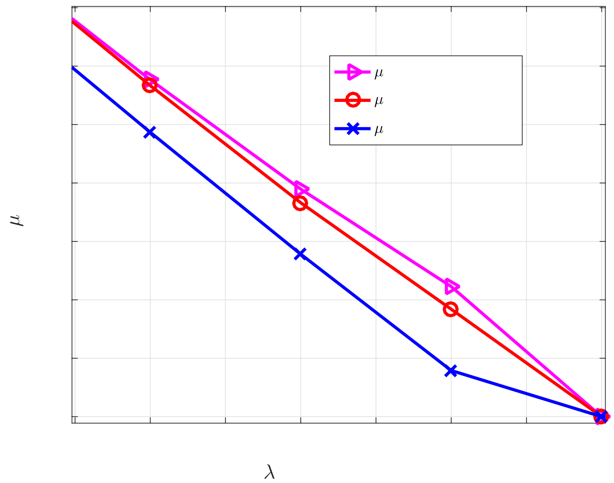

Figure 10: Maximum stable throughput μ_S versus the throughput selected by primary node λ_P.

Fig. 10 shows the the maximum stable throughput μ_S versus the throughput selected by the primary node λ_P. We can see from the figure that over any $\lambda_P < \exp\left(\frac{\beta_P}{\gamma_P}\right) = 0.37$, EA and mutual-information accumulation achieve higher stable throughput of the cognitive link than that without any accumulation, with mutual-information accumulation protocol higher than EA protocol. That is due to increasing the probability of successful primary packets reception at PR, thereby creating more transmission opportunities for ST.

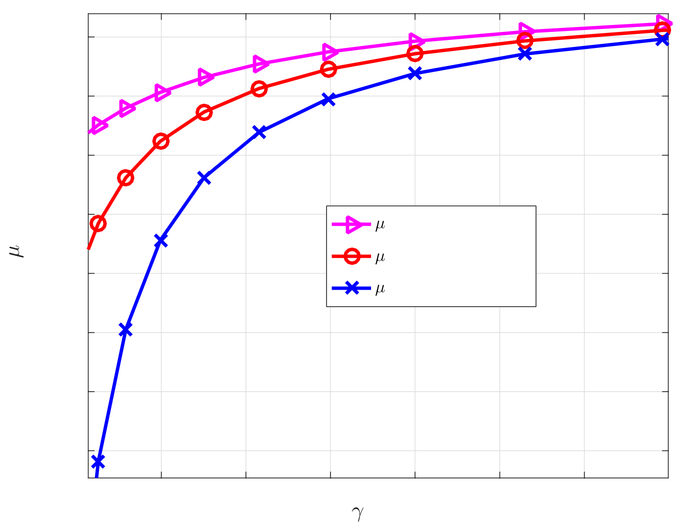

Figure 11: Maximum throughput of the secondary user μ_S versus γ_{SP} ($\lambda_P \approx \exp\left(\frac{\beta_P}{\gamma_P}\right) = 0.37$).

Fig. 11 plots the maximum stable throughput μ_S of the secondary link for varying values of γ_{SP}. As γ_{SP} increases, the relaying gain increases for all the scenarios under study, since most of the traffic is redirected to the secondary link due to the better channel conditions on ST-PR link. Moreover, we can observe that the maximum stable throughput μ_S for EA and mutual-information accumulation protocols achieve higher throughput than that without any accumulation. In addition, the performance of mutual-information accumulation is slightly higher than that of EA when γ_{SP} is low, and the two become similar in performance as γ_{SP} becomes high.

4.2.2 Cooperative Routing for Underlay CRNs using Mutual-Information Accumulation

Fig. 12 gives an example to compare the routing and resource allocation solutions between traditional multi-hop delay-optimal routing without mutual-information accumulation and cooperative routing using mutual-information accumulation in underlay CRNs. All the nodes are distributed in the area of 1×1 (meter ×meter). The PUT is placed at $[0.4, 0.8]$ and the PUR is located at $[0.6, 0.8]$. There are altogether 16 SU nodes in the network: the SU source (node 1) is placed at $[0.1, 0.4]$ and the SU destination (node 16) is located at $[0.9, 0.4]$. The other 14 SU relay nodes are uniformly distributed in the area. The total system bandwidth is set to be $W_T = 1$ Hz and the total system energy is set to be $E_T = 20$ Joule. As shown in The corresponding bandwidth allocation is labeled in the figure. For example, when the source node transmits to node 15, it will use 82% of the total bandwidth due to the interference power constraint. The route for cooperative routing with mutual-information accumulation is $[1, (8,1), (8,3), (8,6), 15, 4, (4,2), 16]$, where the item of $(8, 1)$ means that node 8 and node 1 can be regarded as a virtual node to share PU's spectrum jointly in the second slot. Within this virtual node, node 1 will occupy 54.3% of the PU's spectrum while node 8 will occupy the rest 45.6% of the spectrum. From Fig. 12, we can see that the delay-optimal route of cooperative routing using mutual-information accumulation for underlay CRN is very different from that using traditional multi-hop routing. It is important to note that the cooperative routing and resource allocation solution in [Draper2011Cooperative] can be regarded as a special case of our algorithm by setting $I_T \to \infty$.

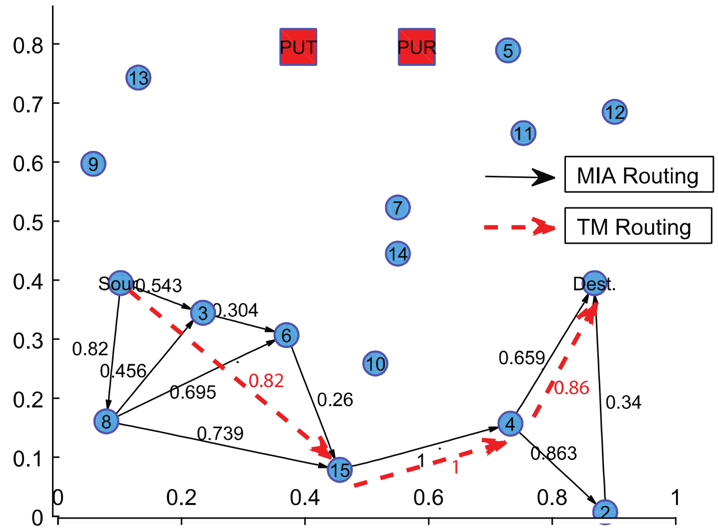

Figure 12: Sample underlay CRN. Delay-optimal cooperative routing using Mutual-Information Accumulation (solid, Mutual-Information Accumulation Routing) and traditional multi-hop delay-optimal routing (dashed, TM Routing).

4.3 Distributed Resource Allocation

4.3.1 Cooperative Retransmission for massive MTC

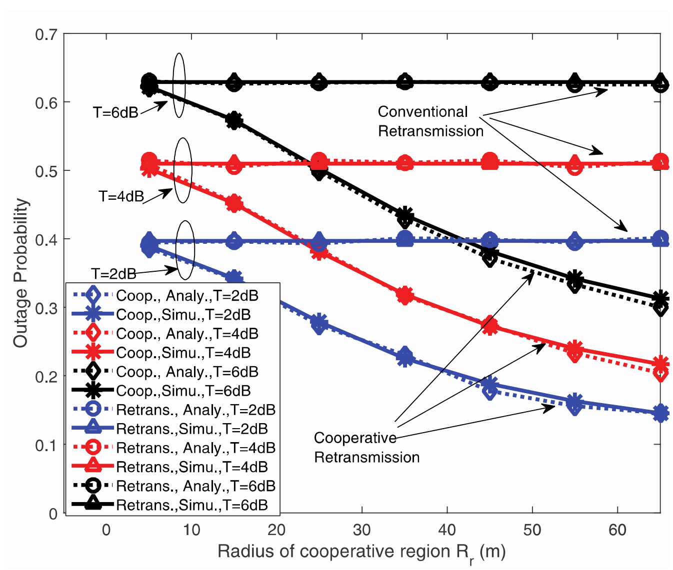

Figure 13: Outage probability as a function of cooperative region.

Fig. 13 shows simulation results as well as numerical results on the probability of outage for both conventional retransmission P^{re} and the proposed cooperative strategy P^{co}. In this figure, each point is an average over 5000 realizations and $\lambda = 10^{-3}m^{-2}$, $p = 0.005$, $\alpha = 4$, and $z =$ 400 m. From Fig. 13, one can see that the introduced cooperative strategy can significantly reduce the outage probability compared to conventional retransmission. Specifically, with a decoding threshold of 2 dB, the outage probability of massive MTC network with cooperative region of 65 m is 14.5% while corresponding conventional retransmission has an outage probability of 39.7%. Note that the outage probability of conventional retransmission is higher than the outage probability of the first time-slot transmission (which is 37.0%) due to the temporally correlated interference. The reason why our introduced cooperative strategy can reduce the outage probability is because: 1) the relay is selected only when it can decode the packet; 2) the selected relay within the cooperative region is much closer to the BS. Furthermore, we can find that as the radius of cooperative region reduces, the outage probability of cooperative communication will approach to the outage probability of conventional retransmission. This is because as the cooperative region reduces, the probability of finding potential relays reduces.

4.3.2 Distribute Cooperative Routing and Resource Allocation in Underlay CRNs

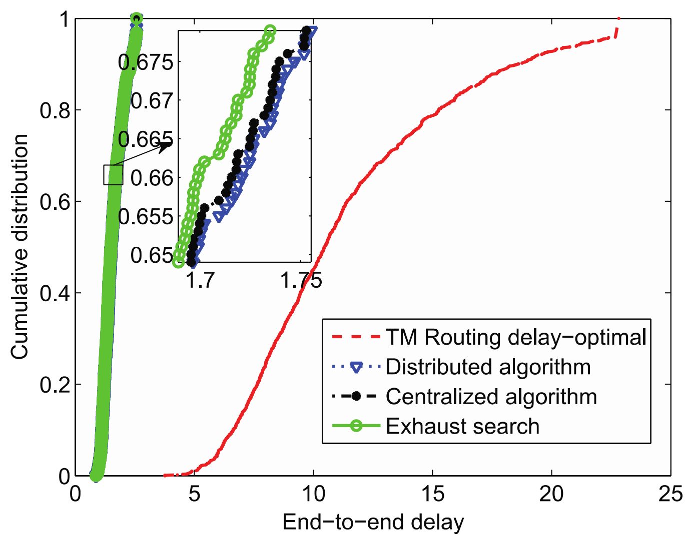

Figure 14: Delay distribution: traditional multi-hop delay-optimal routing, distributed and centralized solution, optimal solution obtained through exhaustive search.

Fig. 14 shows the cumulative delay distribution for the following four approaches: traditional multi-hop delay optimal routing, centralized algorithm for mutual-information accumulation, distributed algorithm for mutual-information accumulation, and optimal algorithm for mutual-information accumulation obtained by exhaustive search. 6 SU nodes are randomly deployed in the network as SU relays. $I_T = 3\text{W}$ and $\alpha = 3$. The average delay of the traditional multi-hop delay-optimal routing is 11.546 sec, while the average delay of centralized and distributed cooperative routing using mutual-information accumulation are 1.620 sec and 1.622 sec, respectively. The optimal delay obtained by exhaustive search is 1.608 sec. On average, both the centralized and distributed cooperative routing algorithms can reduce up to 85.9% of the end-to-end delay compared to traditional multi-hop delay-optimal routing. Furthermore, compared to the optimal route and resource allocation strategies using exhaustive search, our proposed centralized and distributed algorithms only add 0.75% and 0.87% additional delay, respectively. Under the same simulation parameters, if we change the number of SU nodes to 48, the centralized and distributed algorithms can, on average, reduce 77.7% and 77.5% of the end-to-end delay compared to the traditional multi-hop delay-optimal routing. Finally, this simulation figure indicates that the introduced distributed algorithm can obtain almost the same performance on end-to-end delay compared to the centralized algorithm.

4.4 USRP Demo and Graphical User Interface

In June 2015, cooperative routing using rateless coding for a three-node network was demonstrated at the Griffiss Institute using USRP N210s.

Demo Setup: The details of the demo are as follows: 1) 2 laptops controlling 3 USRP N210s; 2) 3 USRP N210s serving as Source, Relay, and Destination; 3) carrier frequency is 2.4 GHz; 4) network bandwidth is 1.25 MHz; 5) sampling rate is 5 Mbps; 6) slot duration for TDMA is 100 ms; and 7) size of Raptor symbol is 2056 bytes with Raptor K = 25. This setup can be seen most clearly in the following figure.

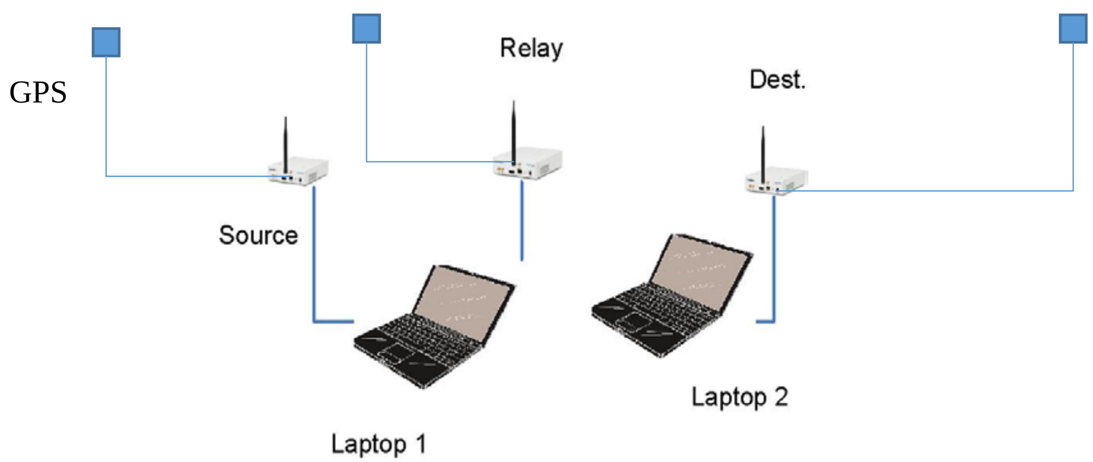

Figure 15: Network Setup for USRP Demo

Medium Access Control (MAC) layer: The frame structure can be seen most clearly in the following figure. It is important to note that the MAC layer control signaling is implemented over the air instead of relying the wired line communication to serve as the control. Due to the wireless control, we need to reserve enough system resource for wireless ACK/NAK to reach the receiver from the transmitter.

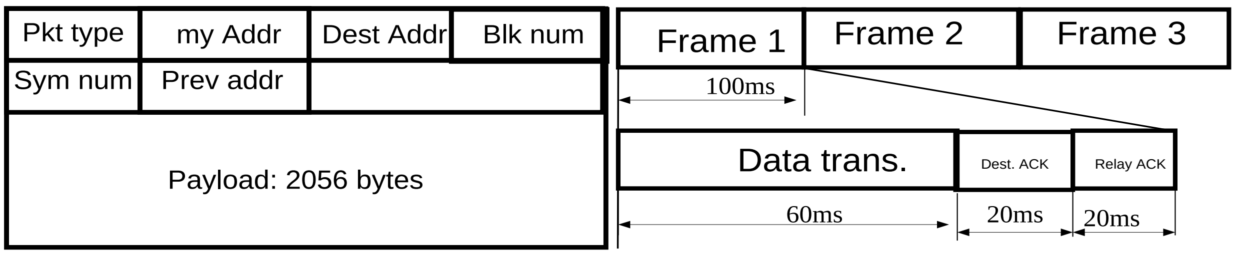

Figure 16: MAC Frame Structure

Graphical User Interface (GUI): GUI design was implemented and demonstrated in May 2016 during the TIM meeting with AFRL. The GUI utilizes remote database (MYSQL) and shows real-time accumulated mutual-information from each transmission. This gives a visual representation of the benefits of rateless coding-based cooperative routing. The developed GUI can be seen more clearly in the following figure.

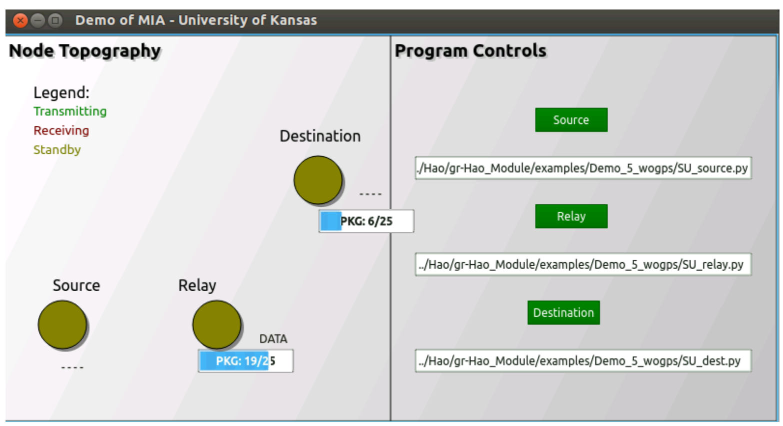

Figure 17: GUI for Cooperative Routing

Demo Outcome: In both demonstrations (June 2015 and May 2016), we showed the following features in different communication layers: 1) Modulation and demodulation, as well as rateless encoder/decoder (RFC5053) at the physical layer; 2) Time division multiple access (TDMA) and routing in the MAC and Network layer; 3) File/image file transfer, live video streaming and GUI/ remote database control in the application layer.

During the USRP demo we showed that the transmission delay/time for non-cooperative communication (from the source to the destination directly) is 57 seconds while the transmission delay/time for the cooperative strategy we developed is 30 seconds. This results a cooperative gain of 1.9 which matches very well with our analytical characterization (2.0).

5.0 CONCLUSIONS

5.1 Spectrum Sensing for Dynamic Spectrum Access Networks

We studied optimal sensing time and power allocation strategies for sensing based spectrum sharing networks subject to a PU's rate loss constraint (RLC) and power constraint. Specifically, in the single-carrier case, we compared the performance (SU's optimal throughput and optimal sensing time) of SBSS with that of spectrum overlay. In the multi-carrier case, we proposed an efficient algorithm to find the optimal sensing time and power allocation. In single-carrier case, SBSS achieved more throughput than spectrum overlay when SUT is far away from PUR or PU can tolerant large rate loss; in multi-carrier case, SBSS achieved higher spectrum efficiency than the corresponding single-carrier case by exploiting additional power allocation flexibility.

5.2 Rateless Coding based Cooperative Dynamic Spectrum Access Networks

Mutual-information accumulation is an enhanced technique to increase the performance of the dynamic spectrum access network. The receiver can decode its packet data if the mutual-information accumulation exceeds a threshold via multiple transmissions from multiple transmitters, and every transmission is useful to contribute some mutual information. In practice, mutual-information accumulation can be realized through rateless codes in which the transmitter generates unlimited number of encoded packets, such that the receiver can decode the data after receiving a sufficient number of encoded packets, irrespective of which ones it has received. This improves the likelihood and ability of multiple nodes to cooperatively serve users and improve DSA network performance.

From the description of the mutual-information accumulation used in CRN to improve the throughput of the network, and minimize the end-to-end delay in multi-hop underlay CRN, we found that mutual-information accumulation outperforms the others significantly. In specific, applying mutual-information accumulation in CRN, where SUs can decode and relay the packets of PUs, performs best compared with energy accumulation and without accumulation scenarios. Also, mutual-information accumulation was used to find optimal routing and resource allocation scheme to minimize the end-to-end delay of the second users while the QoS of primary users are guaranteed. The end-to-end delay was reduced up to 85.9% compared with the traditional scheme without mutual-information accumulation [Chen2015Cooperative].

5.3 Distribute Resource Allocation

Centrally determining resource allocation for all candidate transmission nodes in a large-scale network, if even possible, is an exceedingly expensive operation. A potential solution is to perform distributed resource allocation in which the resource allocation is determined locally. In a distributed resource allocation scheme, a node does not need to know the information of the whole network, instead it makes a decision based only on the information of its own and surrounding nodes. Also, if one node is out of charge, then a new node can be found locally, and quickly. Compared with the centralized resource allocation, the distributed scheme is a quite cost-efficient, flexible, and robust, and is widely used in many research fields such as massive MTC and cooperative routing in multi-hop CRNs.

In MTC networks, the inactive MTDs were allowed to act as relays for outage MTDs. Using point process theory, appropriate relay MTDs were selected to minimize the outage probability of this kind of massive MTC network. Both numerical and simulation results demonstrated the great promise of cooperation of the relay MTD and the source MTD in massive MTC networks.

In cooperative routing multi-hop CRNs, an efficient distributed routing and resource allocation scheme was proposed, and it was shown that the complexity of the distributed scheme was lower than the centralized scheme. Simulation results showed that the performance of the distributed scheme is very close to the centralized scheme.

5.4 USRP Hardware Demo

Hardware demonstrations using USRP N210s were conducted during two TIMs in AFRL. The basic features of the rateless coding-based cooperative routing were implemented in GNU radio and the protocols in almost all communication layers (from PHY to APP) were changed. The demo showed that performance gains of rateless coding-based cooperative routing were realistic and achieved in practice. Furthermore, the achieved performance gain matched very well to theoretical results.

6.0 REFERENCES

[Abdelkader2013 SGBR] T. Abdelkader, K. Naik, A. Nayak, N. Goel, and V. Srivastava, “SGBR: A routing protocol for delay tolerant networks using social grouping,” *IEEE Trans. Parallel Distrib. Syst.*, vol. 24, no. 12, pp. 2472–2481, Dec 2013

[Andrews 2014 What] J. Andrews, S. Buzzi, W. Choi, S. Hanly, A. Lozano, A. Soong, and J. Zhang, “What will 5G be?” *IEEE J. Sel. Areas Commun.*, vol. 32, no. 6, pp. 1065–1082, June 2014.

[Caleffi2012OPERA] M. Caleffi, I. Akyildiz, and L. Paura, “OPERA: Optimal routing metric for cognitive radio ad hoc networks,” *IEEE Trans. Wireless Commun.*, vol. 11, no. 8, pp. 2884–2894, Aug. 2012.

[Castura2007Rateless] J. Castura and Y. Mao, “Rateless coding for wireless relay channels,” *IEEE Trans. Wireless Commun.*, vol. 6, no. 5, pp. 1638–1642, May 2007.

[Chen2012A] H. Chen, P. Ren, L. Sun, and Q. Du, “A distributed routing and timeslot assignment algorithm for cognitive radio ad hoc networks with primary-user protection,” in *Proc. ICST CHINACOM*, Kunming, China, Aug. 2012, pp. 470–474

[Chen2015Optimal] H. Chen, L. Liu, J. D. Matyjas, and M. J. Medley, “Optimal resource allocation for sensing-based spectrum sharing D2D networks,” *Comput. & Electr. Eng.*, vol. 44, no. Supplement C, pp. 107 – 121, 2015.

[Chen2015Cooperative] H. Chen, L. Liu, J. D. Matyjas, and M. J. Medley, “Cooperative routing for underlay cognitive radio networks using mutual-information accumulation,” *IEEE Trans. Wireless Commun* vol. 14, no. 12, pp. 7110-7122, Dec. 2015.

[Chowdhury2011CRP] K. Chowdhury and I. Akyildiz, “CRP: A routing protocol for cognitive radio ad hoc networks,” *IEEE J. Sel. Areas Commun.*, vol. 29, no. 4, pp. 794–804, Apr. 2011.

[Devroye2006Achievable] N. Devroye, P. Mitran, and V. Tarokh, “Achievable rates in cognitive radio channels,” *IEEE Trans. Inf. Theory*, vol. 52, pp. 1813–1827, May 2006.

[Dhillon2014Fundamentals] H. S. Dhillon, H. Huang, H. Viswanathan, and R. A. Valenzuela, “Fundamentals of throughput maximization with random arrivals for M2M communications,” *IEEE Trans. Commun.*, vol. 62, no. 11, pp. 4094–4109, Nov 2014.

[Dhillon2015Wide] H. S. Dhillon, H. C. Huang, and H. Viswanathan, “Wide-area wireless communication challenges for the internet of things,” *CoRR*, vol. abs/1504.03242, 2015

[Molisch2007Performance] A. Molisch, N. Mehta, J. Yedidia, and J. Zhang, "Performance of Fountain Codes in Collaborative Relay Networks", *IEEE Trans. on Wireless Commun.*, vol. 6, no. 11, pp. 4108–4119, Nov. 2007.

[Zhao2005Practical] B. Zhao and M. Valenti, "Practical Relay Networks: A Generalization of Hybrid-ARQ", *IEEE J. on Sel. Areas Commun.* (JSAC), 23(1):7–18, Jan. 2005.

[Draper2011Cooperative] S. Draper, L. Liu, A. Molisch, and J. S. Yedidia, “Cooperative transmission for wireless networks using mutual-information accumulation,” *IEEE Trans. Inf. Theory*, vol. 57, no. 8, pp. 5151–5162, Aug 2011.

[ElAzzouni2015Fullduplex] S. ElAzzouni, O. Ercetin, A. El-Keyi, T. ElBatt, and M. Nafie, “Fullduplex cooperative cognitive radio networks,” in *IEEE WiOpt*, pp. 475–482, May 2015.

[Erez2012Rateless] U. Erez, M. Trott, and G. W. Wornell, “Rateless coding for gaussian channels,” *IEEE Trans. Inf. Theory*, vol. 58, no. 2, pp. 530–547, Feb. 2012

[Ganti2012Spatial] R. Ganti and M. Haenggi, “Spatial analysis of opportunistic downlink relaying in a two-hop cellular system,” *IEEE Trans. Commun.*, vol. 60, no. 5, pp. 1443–1450, May 2012.

[Haenggi2013Diversity] M. Haenggi and R. Smarandache, “Diversity polynomials for the analysis of temporal correlations in wireless networks,” *IEEE Trans. Wireless Commun.*, vol. 12, no. 11, pp. 5940–5951, November 2013.

[Hamdi2009Power] K. Hamdi and K. Ben Letaief, “Power, sensing time, and throughput tradeoffs in cognitive radio systems: A cross-layer approach,” in *Proc. Wireless Communications and Networking Conference, 2009*, April 2009, pp. 1–5.

[Ho2012Energy] C. Y. Ho and C. Y. Huang, “Energy-saving massive access control and resource allocation schemes for M2M communications in OFDMA cellular networks,” IEEE Wireless Commun. Lett., vol. 1, no. 3, pp. 209–212, June 2012.

[Kang2009Sensing] X. Kang, Y.-C. Liang, H. Garg, and L. Zhang, “Sensing-based spectrum sharing in cognitive radio networks,” *IEEE Trans. Veh. Technol.*, vol. 58, no. 8, pp. 4649–4654, Oct 2009.

[Kang2010Optimal] X. Kang, H. Garg, Y.-C. Liang, and R. Zhang, “Optimal power allocation for ofdm-based cognitive radio with new primary transmission protection criteria,” *IEEE Trans. Wireless Commun.*, vol. 9, no. 6, pp. 2066–2075, June 2010.

[Liang2008Sensing] Y.-C. Liang, Y. Zeng, E. Peh, and A. T. Hoang, “Sensing-throughput tradeoff for cognitive radio networks,” *IEEE Trans. Wireless Commun.*, vol. 7, no. 4, pp. 1326–1337, April 2008.

[Luby2002LT] M. Luby, “LT codes,” in *Proc. IEEE FOCS*, 2002, pp. 271–280.

[Neely2005Dynamic] M. Neely, E. Modiano, and C. Rohrs, “Dynamic power allocation and routing for time-varying wireless networks,” *IEEE J. Sel. Areas Commun.*, vol. 23, no. 1, pp. 89–103, Jan. 2005.

[Nigam2015Spatiotemporal] G. Nigam, P. Minero, and M. Haenggi, “Spatiotemporal cooperation in heterogeneous cellular networks,” *IEEE J. Sel. Areas Commun.*, vol. 33, no. 6, pp. 1253–1265, June 2015.

[Rem2014Cad] P. Ren, Y. Wang, and Q. Du, “Cad-mac: A channel-aggregation diversity based mac protocol for spectrum and energy efficient cognitive adhoc networks,” *IEEE J. Sel. Areas Commun.*, vol. 32, no. 2, pp. 237–250, February 2014.

[Palanki2004Rateless] R. Palanki and J. S. Yedidia, “Rateless codes on noisy channels,” in *Proc. IEEE ISIT*, Chicago, IL, USA, Jun. 2004, pp. 38–38.

[Pei2009How] Y. Pei, Y.-C. Liang, K. Teh, and K. H. Li, “How much time is needed for wideband spectrum sensing?” *IEEE Trans. Wireless Commun.*, vol. 8, no. 11, pp. 5466–5471, November 2009.

[Sharma2008Channel] M. Sharma, A. Sahoo, and K. D. Nayak, “Channel modeling based on interference temperature in underlay cognitive wireless networks,” in *Proc. Wireless Communication Systems. 2008. IEEE International Symposium on*, Oct 2008, pp. 224–228.

[Shi2012Joint] C. Shi, Y. Wang, and P. Zhang, “Joint spectrum sensing and resource allocation for multi-band cognitive radio systems with heterogeneous services,” in *Proc. Global Communications Conference (GLOBECOM), 2012 IEEE*, Dec 2012, pp. 1180–1185.

[Shokrollahi2006Raptor] A. Shokrollahi, “Raptor codes,” *IEEE Trans. Inf. Theory*, vol. 52, no. 6, pp. 2551–2567, Jun. 2006.

[Simeone2007Stable] O. Simeone, Y. Bar-Ness, and U. Spagnolini, “Stable throughput of cognitive radios with and without relaying capability,” *IEEE Trans. Commun.*, vol. 55, pp. 2351–2360, Dec 2007.

[Su2010Active] W. Su, J. Matyjas, and S. Batalama, “Active cooperation between primary users and cognitive radio users in cognitive ad-hoc networks,” in *Proc. Acoustics Speech and Signal Processing (ICASSP), 2010 IEEE International Conference on*, March 2010, pp. 3174–3177.

[Stotas2011Optimal] S. Stotas and A. Nallanathan, “Optimal sensing time and power allocation in multiband cognitive radio networks,” *IEEE Trans. Commun.*, vol. 59, no. 1, pp. 226–235, January 2011.

[Urgaonkar2012Optimal] R. Urgaonkar and M. J. Neely, “Optimal routing with mutual information accumulation in wireless networks,” *IEEE J. Sel. Areas Commun.*, vol. 30, no. 9, pp. 1730–1737, Oct. 2012.

[Xie2013To] C. Xie, K. C. Chen, and X. Wang, “To hop or not to hop in massive machine-to-machine communications,” in Wireless Communications and Networking Conference (WCNC), 2013 IEEE, April 2013, pp. 1021–1026.

[Zhang2013On] X. Zhang et al., “On the study of outage performance for cognitive relay networks (CRN) with the nth best-relay selection in rayleigh-fading channels,” *IEEE Wireless Commun. Lett.*, vol. 2, pp. 110–113, Feb 2013.

APPENDIX – PUBLICATIONS AND PRESENTATIONS

PUBLICATIONS

- R. Atat, J. Ma, H. Chen, U. Lee, J. Ashdown, and L. Liu, "Cognitive Relay Networks with Energy and Mutual-Information Accumulation", submitted *IEEE Intl. Workshop on Wireless Commun. and Networking in Extreme Environments* (WCNEE) 2018.
- H. Chen, L. Liu, S. Puddlewski, M. Medley, and J. Matyjas, "Mutual Information Accumulation over Random Wireless Ad-Hoc Networks", submitted to 2018 *IEEE Intl. Conf. on Commun.* (ICC), May 2018.
- R. Atat, L. Liu, J. Ashdown, M. Medley, J. Matyjas, and Y. Yi, "Improving Spectral Efficiency of D2D Cellular Networks Through RF Energy Harvesting", 2016 *IEEE Global Commun. Conf.* (GLOBECOM' 16). (**Best Paper Award**)
- R. Atat, L. Liu, J. Ashdown, M. Medley, and J. Matyjas, "On the Performance of Relay-Assisted D2D Networks under Spatially Correlated Interference", 2016 *IEEE Global Commun. Conf.* (GLOBECOM' 16).
- R. Atat, H. Chen, L. Liu, J. Ashdown, M. Medley, and J. Matyjas, "Fundamentals of Spatial RF Energy Harvesting for D2D Cellular Networks", 2016 *IEEE Global Commun. Conf.* (GLOBECOM' 16).
- S. Mosleh, J. Ashdown, J. Matyjas, M. Medley, J. Zhang, and L. Liu, "Interference Alignment for Downlink Multi-Cell LTE-Advanced Systems With Limited Feedback", *IEEE Trans. Wireless Commun.*, vol. 15, no. 12, pp. 8107-8121, Dec. 2016.
- H. Chen, L. Liu, T. Novlan, J. Matyjas, B. Ng, and J. Zhang, "Spatial Spectrum Sensing-Based Device-to-Device (D2D) Cellular Networks", *IEEE Trans. Wireless Commun.*, vol. 15, no. 11, pp. 7299-7313, Nov. 2016.
- H. Chen, R. Shafin, R. Atat, Y. Yi, and L. Liu, "Performance Analysis on Nano-Networks: A Stochastic Geometry Approach". 2016 *ACM Intl. Conf. on Nanoscale Computing and Commun.*, Article 36, Sep. 2016.
- H. Chen, L. Liu, J. Matyjas, and M. Medley, "Cooperative transmission for cognitive radio networks using mutual-information accumulation," *IEEE Trans. Wireless Commun.*, vol. 14, no.12, pp.7110-7122, Dec. 2015
- H. Chen, L. Liu, J. Matyjas, and M. Medley, "Optimal resource allocation for sensing-based spectrum sharing D2D networks," the special issue on "*Emerging Technologies for Internet of Things*" at the *Elsevier Journal of Computers and Electrical Engineering*, vol. 44, pp. 107-121, May 2015.

- H. Chen, L. Liu, J. Matyjas, and M. Medley, “Optimal resource allocation for sensing based spectrum sharing cognitive radio networks,” **in *Proc*.** 2014 *IEEE Global Communications Conference (GLOBECOM)*, pp. 899–904, Dec. 2014(Austin, TX, USA).
- L. Liu, H. Chen, J. Matyjas, and M. Medley, "Cooperative transmission for cognitive radio networks using mutual-information accumulation", **in *Proc*.** 2014 *IEEE* Wireless and Optical Communication Conference (WOCC), pp.1-5, May 2014(Newark, NJ, USA).

PRESENTATIONS:

"Cooperative Routing for Underlay Cognitive Radio Networks using Rateless Codes", NSF I/UCRC BWAC Industrial Advisory Board meeting, South Bend, IN, USA, Oct. 2017.

"On the Performance of Relay-Assisted D2D Networks under Spatially Correlated Interference", 2016 *IEEE Global Commun. Conf.* (GLOBECOM’ 16), Washington, DC USA, Dec. 2016.

"Performance Analysis on Nano-Networks: A Stochastic Geometry Approach". 2016 *ACM Intl. Conf. on Nanoscale Computing and Commun.*, Boston, MA, USA, Sep. 2016.

"Updates on Cooperative Routing for Dynamic Aerial Layer Networks", AFRL Technical Interchange Meeting, Rome, NY, USA, May 2016.

"Progress and Updates on Cooperative Routing for Dynamic Aerial Layer Networks", AFRL Technical Interchange Meeting, Rome, NY, USA, June 2015.

"Optimal resource allocation for sensing based spectrum sharing cognitive radio networks", 2014 *IEEE Global Communications Conference (GLOBECOM)*, Austin, TX, USA, Dec. 2014.

"Cooperative transmission for cognitive radio networks using mutual-information accumulation", 2014 *IEEE* Wireless and Optical Communication Conference (WOCC), Newark, NJ, USA, May 2014.

"Cooperative Routing for Dynamic Aerial Layer Networks", AFRL Project Kickoff Meeting, Feb. 2014.

LIST OF SYMBOLS, ABBREVIATIONS, AND ACRONYMS

ARQ	automatic repeat request
BS	base station
CRN	cognitive radio network
CSI	channel state information
DAS	dynamic spectrum access
D2D	device-to-device
EA	energy accumulation
LP	linear programming
MTC	machine type communication
MTD	machine type device
PST	power spectrum density
PT	primary transmitter
PR	primary receiver
PU	primary user
PUR	primary user receiver
PUT	primary user transmitter
QoS	quality of service
RLC	rate loss constraint
SBSS	sensing based spectrum sharing
ST	secondary transmitter
SR	secondary receiver
SU	secondary user

SUR	secondary user receiver
SUT	secondary user transmitter